DIAGNOSIS OF MATRIX QUALITY IN CVD INFILTRATED CARBON-CARBON BY IN-PROCESS MONITORING AND NONDESTRUCTIVE EVALUATION

E. R. Stover and J. A. Roetling
General Electric Company, Re-Entry and Environmental Systems Division
Philadelphia, Pa. 19101

Introduction

A carbon-carbon composite material developed for re-entry applications utilizes a 3-D orthogonal preform, comprising about one-half of the volume, which is initially CVD infiltrated and surface ground before adding a graphite matrix. Impregnation with pitch and carbonization above 600°C at 100 MPa, followed by graphitization to 2750°C, provides adequate densification in 4 to 6 cycles. Ablation tests have shown that performance varies with matrix quality, particularly residual porosity, which can vary due to thermal history during the pressure bake. Procedures were developed to monitor the material during successive process cycles and to evaluate porosity distribution in the finished billets nondestructively.

Gradients in Density and Porosity

The isothermal CVD infiltration of the preforms (typically 10x10x20 cm) results in an initially high density at the surface, which develops a lower final density compared with the billet core, because CVD films on the filaments block penetration of pores in the fiber bundles by the pitch. Figure 1 illustrates porosity data obtained on samples cut from different locations in billets, using either liquid or gas permeation. Normally, open porosity as well as density is lower near the surface. However, in some samples (upper left in Fig. 1), low density in the core was associated with high open porosity, apparently as a result of bubble formation in the impregnant within the billets during the autoclave processing.

Measurements during Processing

Most of the processing discussed here was conducted at the Y-12 Plant, Union Carbide Corp. Nuclear Div., Oak Ridge, Tenn., where the cycles were first developed, and at the Battelle Columbus Laboratories. Later cycles at GE-RESD were accomplished with thermocouples placed within billets or adjacent pitch; these data showed a significant thermal lag compared with autoclave chamber temperatures, which had been used to control the pressure-impregnation-carbonization cycles in earlier processing.

Weight and dimension data on each billet, provided to GE-RESD after each process step, provided a basis for evaluating the adequacy of autoclave heating in the absence of accurate material temperature data. The density increase in each cycle followed a consistent trend with the available open porosity, as illustrated by Figure 2. The billets in one run had abnormally high densities, shown in the figure, because of a heater failure, and weight loss during subsequent graphitization was high. The "coke" lost in graphitization, calculated by dividing the weight lost during graphitization by the weight gained in the preceding autoclave cycle is shown as % CLIG in the figure. Even in normal runs, this factor varied with location of billets in the autoclave and with the size of the load, indicating differences in maximum temperature in the material even though cycles were nominally the same. When the cycle was modified to provide additional time at maximum temperature and pressure, lower "CLIG" values confirmed that billets had reached higher temperatures.

Work sponsored by the Air Force Materials Laboratory, Wright-Patterson Air Force Base, Ohio.

3-Dimensional Radiometry

Unusual heating conditions in one autoclave resulted in abnormalities not adequately detected by changes in weight and density. Subsequent studies with many thermocouples in a can have shown that significant temperature gradients can occur. In one set of runs the top half of billets set on end in the can contained a porous core, but the pitch displaced remained in outer portions of the billet, leaving the average bulk density unaffected. This condition was first identified by precision radiometric density apparatus and a 3-dimensional analysis of the data.

Figure 3 illustrates the normal density gradient found in blocks cut from a slab through a billet. "Core" and "edge" average densities represent this gradient. Such densities were calculated from the relative absorption of radiation in a well-collimated 0.64 cm diameter beam, centered at stations representing the centers of equal-sized prisms in the billet, equated to the measured bulk density (Figure 4). For the 10x10 cm section billets, 4 rows on both "X" and "Y" faces were normally used, although 8 rows combined with "Z" direction data have been used to establish the gradients with better precision. The reproducibility of the procedure and adequacy of the counting statistics at each station have been established by evaluating billets without CVD in which the true gradients are small. A simple analysis of the in-line density gradients to evaluate core vs. edge density has been refined by an iterative computer program which provides the best set of densities for all of the internal prism positions (usually cubes) matching the measured absorptions at each station.

Figure 5 illustrates core vs. edge density averages down the length of both normal and abnormal billets, which also provided samples for some of the density and porosity comparisons in Figure 1. Good agreement has been found between measured densities of core samples and those predicted from the radiometry, providing confidence in the nondestructive evaluation of porosity gradients in this material.

Acknowledgments: W. Mueller, A. E. Oaks, T. M. Hollenbeck and D. G. Breskman, G. E.; Maj. H. E. Keck, AFML; R. Paluzelle, Y-12, UCCND, and W. Chard, Battelle Columbus Laboratories, made particularly significant contributions to this work.

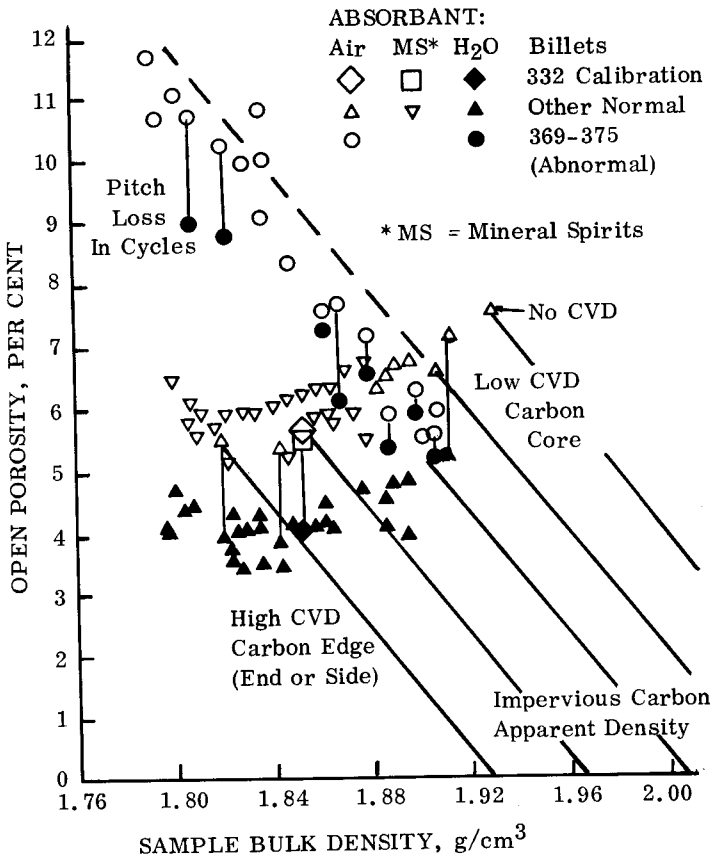

Fig. 1. Comparative Open Porosity Data Obtained by Different Methods, and Densities in Different Billet Locations. (MS Data provided by H. Littleton, Southern Research Institute.)

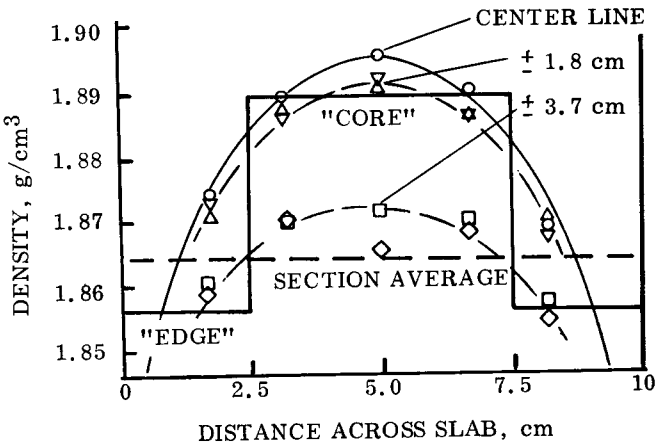

Fig. 3. Bulk Density of 25 (5x5) Blocks in a Slab, and Average "Edge" and "Core" Densities.

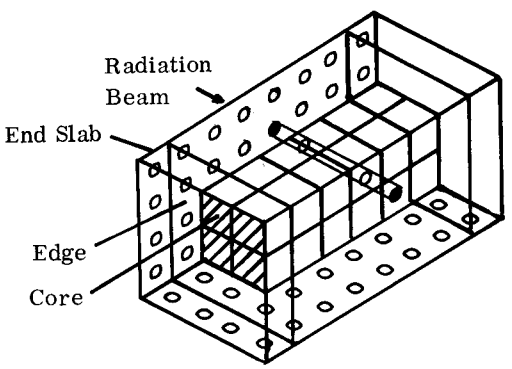

Fig. 4. Typical Stations for Radiometric Analysis Showing Calculated "Core".

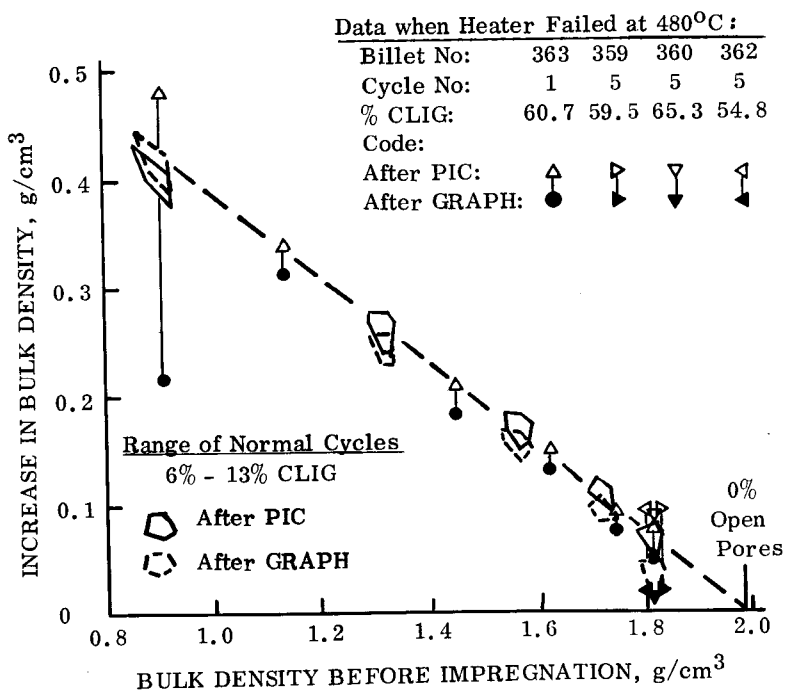

Fig. 2. Densification in Normal and Abnormal Cycles.

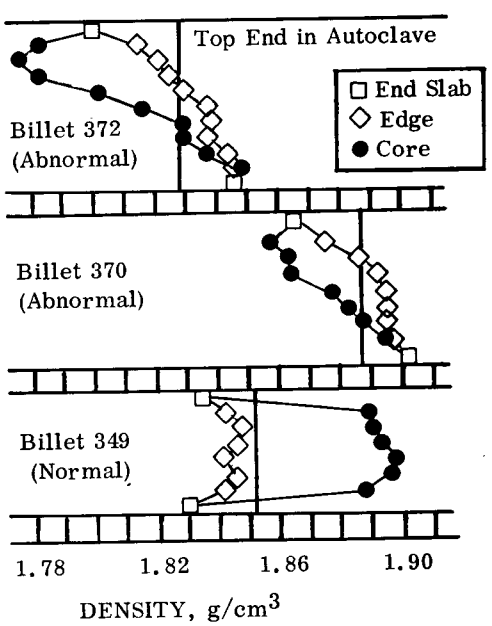

Fig. 5. Radiometric Edge and Core Densities at 2.54 cm Stations along the Length of Billets. Bar is Billet Average.